Two- and Three-Dimensional Validation of Icing Model

***Ryosuke Hayashi[1] and Makoto Yamamoto[2]**

[1]Graduate School of Mechanical Engineering, Tokyo University of Science
6-3-1 Niijyuku, Katsushika-ku, Tokyo, Japan
[2]Department of Mechanical Engineering, Tokyo University of Science

*Corresponding author: j4512703@ed.tus.ac.jp

Abstract

Ice accretion is a phenomenon where super-cooled water droplets impinge and accrete on a body. It occurs frequently on airplanes, windmills and conductor cables. In particular, when ice layer is formed on an aircraft wing, it affects on the aerodynamic performance by increasing drag and decreasing lift, and it may cause a serious accident. On a jet engine, ice accretion disturbs the inlet flow, and separated ice pieces can damage to the compressor and the casing, which leads to the severe performance degradation. There have been several accidents due to the ice accretion. Therefore, the estimation of ice accretion in the design phase is necessary to avoid accidents. The research on ice accretion phenomena has been conducted since early 1990's. The first icing simulation model was developed by Messinger in 1953. This model has been widely used in simulating ice accretion phenomena. Recently, Extended Messinger model was developed by Ozgen and Canibek in 2009. This model is more sensitive than Original Messinger model in suitably estimating the runback mass. The predictive performance for the runback mass has a huge influence on ice accretion phenomena in glaze ice condition. In this study, we conducted the validation of these icing models in two- and three-dimensional field. Finally, we indicated Extended Messinger model is more superior to Original Messinger model in simulating glaze icing.

Keywords: Multiphysics CFD, Ice Accretion, Jet Engine, Messinger Model

Introduction

Ice accretion is a phenomenon where super-cooled water droplets impinge and accrete on a body. It has two types of ice shape. One is called ‘rime ice’ which is generated at very low temperature (less than -10 °C). On the rime ice condition, droplets in the air instantly freeze at the impingement point. The other is called ‘glaze ice’ which is generated at -10 to 0 °C. On the glaze ice condition, droplets gradually freeze with running along a body (so-called runback). This phenomenon is considerably important in simulating the glaze icing.

When ice layer is formed on an aircraft wing, it affects on the performance by increasing drag and reducing lift, and it may cause a serious accident. On a jet engine, ice accretion disturbs the inlet flow, and separated ice pieces can damage to the compressor and the casing, which leads to the severe performance degradation. There have been several instances of accidents due to ice accretion. Obviously, it is essential that the mechanisms of ice accretion are understood. The estimation of ice accretion is necessary to avoid accidents and useful to reduce the cost and the design time in the design phase of aircrafts and jet engines. However, the experimental investigations are very difficult, because it is not easy to set ice accretion conditions repeatedly in a wind tunnel. Therefore, it is expected computational fluid dynamics (CFD) will be a useful way to predict ice accretion phenomenon. CFD research of ice accretion phenomena has widely been conducted by agencies and universities, such as NASA [1], ONERA [2] and so on.

The first icing simulation model was developed by Messinger in 1953 [3]. This Original Messinger model has been widely used in the major research institution such as NASA, DRA and ONERA. The results predicted with the Original Messinger model is in good agreement with the experimental data in rime ice conditions. However, in glaze ice conditions, the predictive performance of the Original Messinger model is low, because the mass of the runback is underestimated. Therefore, the user specially modified the Original Messinger model in simulating glaze icing phenomena. Recently, Extended Messinger model was developed by Ozgen and Canibek in 2009. It is expected that the Extended Messinger model is more sensitive to glaze ice conditions than Original Messinger model, because it includes phase change condition from rime ice to glaze ice. However, the extended Messinger model has not been extensively validated yet.

In this study, we conducted the validation of these icing models two- and three-dimensional field. In the two-dimensional validation, we adopted the NACA 0012 airfoil because a lot of experimental data are available. In the three-dimensional validation, we adopted a fan rotor and FEGVs, because these components are easy to accrete ice. Finally, we indicated Extended Messinger model is more superior to Original Messinger model in simulating glaze icing.

Numerical Procedure

Our icing simulation code is composed of iterative computations for fluid motion, droplet trajectory, thermodynamics and grid modification. Below each computational detail is explained.

Flow Field

The flow field is assumed to be three-dimensional, compressible and turbulent. The governing equations are Favre-averaged continuity, Navier-Stokes and energy equations. Coriolis force and centrifugal force are added as body forces. The Kato-Launder k-ε turbulence model (Kato and Launder, [4]) is applied to estimate turbulence. The governing equations are discretized using second-order upwind TVD scheme (Yee and Harten, [5]) for the inviscid terms, second-order central difference scheme for the viscous ones, and LU-ADI scheme (Fujii and Obayashi, [6]) for the time integration.

Droplet Trajectory

Droplet trajectory calculation based on a Lagrangian approach is performed to obtain the droplet collection efficiency on a body. The calculation uses the following assumptions:

1. Droplet is spherical.
2. Droplet is sufficiently small, and thus it does not break up.
3. Forces acting on the droplet are drag, centrifugal force and Coriolis force.
4. Droplets do not interact with each other.
5. Droplets do not affect on the flow field (one-way coupling).
6. Initial droplet velocity is equal to the gas velocity at the release point.

The equation of droplet motion is

$$\frac{d\vec{U}_d}{dt} = \frac{3}{4} C_D \frac{\rho_f}{\rho_d} \frac{1}{d_d} \vec{U}_r \left| \vec{U}_r \right| - \left\{ 2\vec{\Omega} \times \vec{U}_d - \vec{\Omega} \times \left(\vec{\Omega} \times \vec{r}_d \right) \right\} \tag{1}$$

where t is the time, U_r is the relative velocity between the gas and the droplet, d_d is the droplet diameter, and ρ_f and ρ_d are the gas and the droplet density. The second term on the RHS represents

the centrifugal force and Coriolis force, where Ω is the rotational speed, and r_d is the radial position of the droplet. The drag coefficient C_D is expressed as:

$$C_D = \frac{24}{\mathrm{Re}_d}\left(1 + 0.15\,\mathrm{Re}_d^{\,0.687}\right) \tag{2}$$

where Re_d is the Reynolds number of the droplet based on the diameter and the relative velocity between the gas and the droplet.

The droplet trajectory calculation is conducted to obtain the collection efficiency. The collection efficiency β is followed as:

$$\beta = \frac{A_{in} U_{in} LWC}{\rho_d MVD} \frac{N_{imp}}{N_{in} A_{imp}} \tag{3}$$

where A_{in} is the droplet inlet area, U_{in} is the droplet inlet velocity, LWC is the liquid water content, N_{imp} is the droplet impingement number, N_{in} is the droplet inlet number and A_{imp} is the droplet impingement area. The collection efficiency is one of the key parameters of the icing simulation.

Original Messinger Model

The Original Messinger model was developed by Messinger in 1953. This model is based on the mass and energy balance in a control volume. The governing equations is followed as:

$$m_{im} + m_{in} = m_{ac} + m_{e,s} + m_{out} \tag{4}$$

$$Q_{im} + Q_{in} + Q_{air} + Q_{fri} = Q_{ac} + Q_{e,s} + Q_{out} + Q_{con} \tag{5}$$

where m_{im}, m_{in}, m_{ac}, m_{out} and $m_{e,s}$ are the mass of impingement , runback-in, accretion, evaporating (or sublimating) and runback-out, respectively; Q_{im}, Q_{in}, Q_{air}, Q_{fri}, Q_{ac}, $Q_{e,s}$, Q_{out} and Q_{con} are the energy of impingement, runback-in, air, friction, accretion, evaporating (or sublimating), runback-out and convection. The freezing rate f can be derived from Eqs. (4) and (5).

$$f = \frac{m_{ac}}{m_{im} + m_{in}} \tag{6}$$

$$m_{out} = (1 - f)(m_{im} + m_{in}) - m_{e,s} \tag{7}$$

if f = 1, all mass in the control volume accretes, on the other hand, if f = 0, all mass in the control volume runbacks to the next cell.

Extended Messinger Model

Original Messinger model has a problem in the predictive performance of the runback mass, because the phase change from rime ice to glaze ice is instant. To get over this problem, Extended Messinger model was developed by Orgen and Canibak in 2009 [7]. This model is based on the Stefan problem, which is a standard method of the phase change problem. The governing equations are expressed as:

$$\frac{\partial T_i}{\partial t} = \frac{k_i}{\rho_i C_{pi}} \frac{\partial^2 T_i}{\partial h^2} \tag{8}$$

$$\frac{\partial T_w}{\partial t} = \frac{k_w}{\rho_w C_{pw}} \frac{\partial^2 T_w}{\partial h^2} \tag{9}$$

$$\rho_i \frac{\partial B_i}{\partial t} + \rho_w \frac{\partial B_w}{\partial t} = m_{im} + m_{in} - m_{e,s} \tag{10}$$

$$\rho_i L_F \frac{\partial B_i}{\partial t} = k_i \frac{\partial T_i}{\partial h} - k_w \frac{\partial T_w}{\partial h} \tag{11}$$

where Eqs. (8) and (9) are the energy equations in the ice and water layer respectively, Eq. (10) is the mass conservation equation and Eq. (11) is the phase change condition at the ice/water interface. In these equations, T_i and T_w are the temperatures of ice and water; B_i and B_w are the thicknesses of ice and water layers; k_i and k_w are the thermal conductivities of ice and water; C_{pi} and C_{pw} are the specific heats of ice and water; m_{im}, m_{in} and $m_{e,s}$ are impinging, runback and evaporating (or sublimating) water mass flow rates for a control volume, respectively; ρ_i and ρ_w are the density of ice and water; L_F denotes the latent heat of solidification of water. Ice density is assumed to have two different values for rime ice ρ_r and glaze ice ρ_g. The coordinate h is normal to the wall or ice surface.

Two-dimensional validation

Computational Target and Grid

We adopted a NACA 0012 airfoil in the two-dimensional validation, because a lot of experimental data are available in literatures. In this study, the overset grid method is applied to clarify the icing area around the leading edge, where it is easy to occur icing phenomena. The sub grid resolution is important for icing simulation. We checked relatively grid for the icing simulation by three type sub grids; the coarse grid resolution is 81 x 21, the medium grid resolution is 201 x 51 and the fine grid resolution is 301 x 81. The coarse grid has a margin of error in the icing limit point. Therefore, we adopted the medium grid in this study. The number of grid point in the main grid is 15,691 and that in the sub grid point is 10,251. The computational domain is 20 chord × 20 chord.

Computational Condition

The computational condition is listed in Table 1. The LWC means the liquid water content, and the MVD is the median volume diameter of droplets. The number of validation cases is six. The number of inlet droplets is 1,000,000.The boundary conditions are followed as; in the inlet boundary, the flow angle, the volume flow rate and the total temperature are fixed and the Mach number is extrapolated ; in the outlet boundary, the static pressure is fixed and the others are extrapolated; in the wall boundary, no-slip, adiabatic and wall function conditions are applied. Under the these conditions, we compared Original Messinger model with Extended Messinger model in the two-dimensional validation.

Table 1. Computational Condition of 2D Validation

	Chord [m]	Angle of Attack [deg.]	Velocity [m/s]	Static Temperature [˚C]	Static Pressure [kPa]	LWC [g/m^3]	MVD [μm]	Exposure Time [s]
Run 1	0.530	4.0	58.10	-27.8	95.61	1.30	20.0	480.0
Run 2	0.530	4.0	58.10	-19.8	95.61	1.30	20.0	480.0
Run 3	0.530	4.0	58.10	-13.9	95.61	1.30	20.0	480.0
Run 4	0.530	4.0	58.10	-6.7	95.61	1.30	20.0	480.0
Run 5	0.530	4.0	58.10	-3.9	95.61	1.30	20.0	480.0
Run 6	0.530	4.0	58.10	-2.8	95.61	1.30	20.0	480.0

Result and Discussion

We validated our icing simulation code by use of the NASA, DRA and ONERA simulation data and the experimental data [8]. These simulations were conducted by Original Messinger model. The ice shapes are seen in Fig. 1; (a)-(c) are under the rime ice condition, (d)-(e) are under the glaze ice condition. In the rime ice condition, the noticeable difference of the predictive performance between Original Messinger model and Extended Messinger model does not appear. This is why the runback phenomenon does not occur in the rime ice condition. On the other hand, there is considerable disagreement in the glaze ice condition. Extended Messinger model gives the results closer to the experimental data than Original Messinger model, because it is sensitive to the runback mass. However, the simulation results of NASA, DRA and ONERA can reproduce the glaze icing even if they use Original Messinger model. The reason why our icing simulation code of Original Messinger model is not modified unlike their icing models. Therefore, Original Messinger model need to be modified when simulate the glaze icing.

Three-dimensional validation

Computational Target and Grid

We validated our icing simulation code by use of a jet engine. The icing components of jet engine are the rotor fan, FEGV (fan exit guide vane), nose cone, splitter and low pressure compressor. In this study, we focused on a fan blade and FEGV, because these are more accreted ice area. The jet engine used in this study has twenty-four rotor blades and sixty stator vanes. For simplicity, only one rotor blade and two stator vanes are simulated, assuming the geometrical periodicity. The computational grid based on an overset grid method and a multi block method is exhibited in Fig. 2; (a) is the main

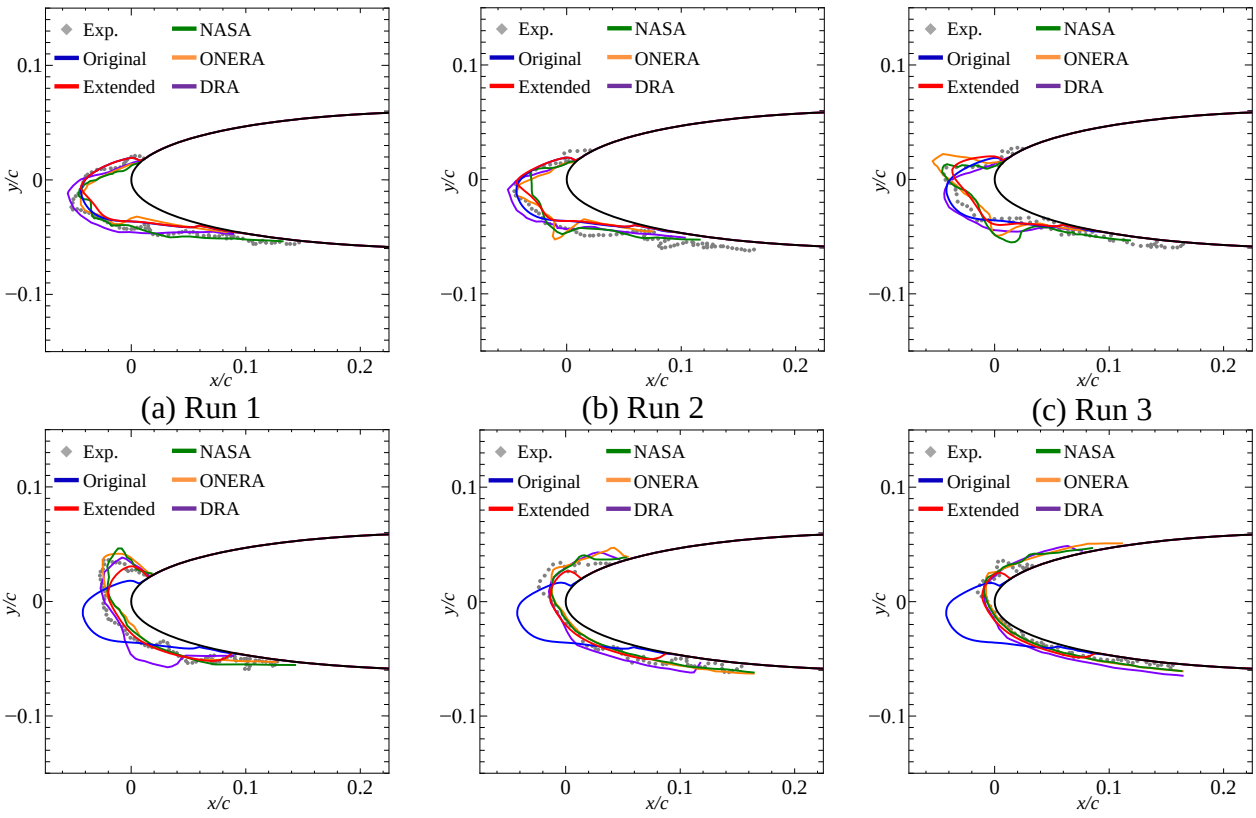

(a) Run 1 (b) Run 2 (c) Run 3

(d) Run 4 (e) Run 5 (f) Run 6

Figure 1. Icing Shape of 2D Validation

grid for the passage, (b) is the sub grid around the blade. The total number of the grid points is about 2.8 million.

Computational Condition

Computational conditions in this study are summarized in Table 2. We set three cases with different total temperature. In all cases, the mass flow rates are same. The droplet trajectory simulations are conducted for 1,000,000 droplets randomly and spatially distributed at the computational upstream boundary. The initial droplet velocity is equal to the local gas velocity. Total pressure, total temperature and flow angle are imposed, and Mach number is extrapolated at the upstream inflow boundary. The inflow turbulent kinetic energy is assumed by the 0.1 % turbulence of the free stream. Adiabatic, no slip and wall function boundary conditions are prescribed on the stationary and rotating surfaces. The exit static pressure is specified.

Result and Discussion

Fig. 3 shows the static temperature distribution at the rotor midspan, which is a pitch-averaged. Around the leading edge of the rotor suction side, the static temperature is considerably low (about 200 K, Run 1) due to the high Mach number region. Even in the high temperature region such as the rotor wake, the stagnation point and the pressure surface on the FEGV, the temperature is below the freezing point. Therefore, ice accretion can occur if the super-cooled droplet impinges on the blade surface.

Fig. 4 indicates the collection efficiency in Run 3. A lot of droplets impinge on the rotor suction side, particularly, at the hub side. There are no impingement droplets on the rotor suction side. Some droplets impinge on the pressure side of the FEGV. Other simulation cases have a same tendency.

Finally, we show numerical results of the ice accretion. Ice thickness distributions are exhibited in Fig. 5. These figures are for the suction side of the rotor fan, because this is the thickest icing area. In all Extended Messinger model cases, icing area expanded to the tip side due to the centrifugal force.

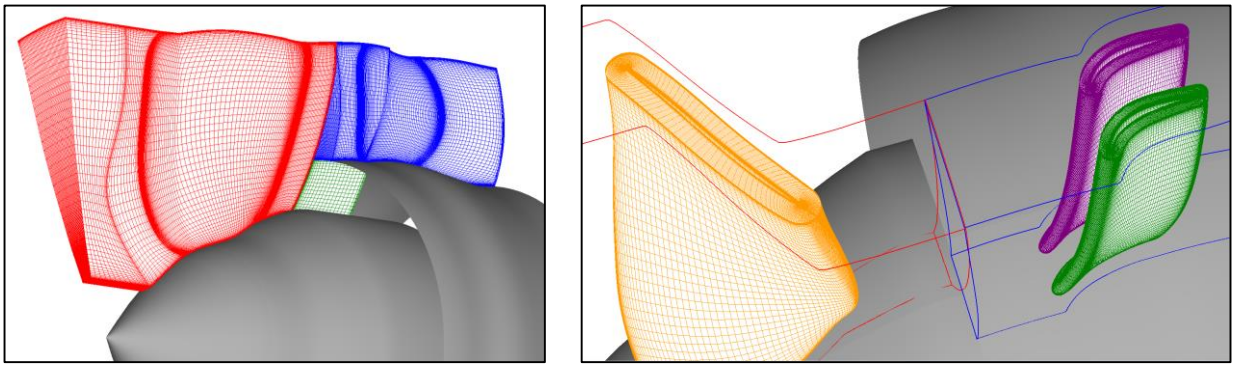

(a) Main Grid (b) Sub Grid

Figure 2. Computational Grid of 3D Validation

Table 2. Computational Condition of 3D Validation

	Rotational Speed [rpm]	Mach Number	Total Pressure [MPa]	Total Temperature [K]	LWC [g/m^3]	MVD [μm]	Exposure Time [s]
Run 1	4291.0	0.44	0.1013	233.15	1.00	20.0	3.0
Run 2	4291.0	0.44	0.1013	243.15	1.00	20.0	3.0
Run 3	4291.0	0.44	0.1013	253.15	1.00	20.0	3.0

This tendency cannot be confirmed by use of Original Messinger model. This is caused by the predictive performance of the runback water. In the case of Extended Messinger model, the higher inlet temperature becomes, the more the runback mass becomes and the larger the icing area is. The ice volumes of all computational conditions are summarized in Fig. 6. In the low inlet temperature case, the icing models make no difference of the ice volume. However, in the high inlet temperature case, the difference between both icing models can be confirmed on the rotor fan icing. On the other hand, the icing on the FEGV is little distinction, because the runback hardly occur at the FEGV. Therefore, we recommend Extended Messinger model in simulating the ice accretion, because this model can reproduce runback phenomena in glaze ice conditions.

Conclusion

We validated Original Messinger model and Extended Messinger model. The knowledge obtained in this study is described below:

(1) In two dimensional validation, the icing model makes no difference on the icing phenomenon in the rime ice condition.
(2) In two dimensional validation, Extended Messinger model is better agreement with the experimental data due to the higher predictive performance of the runback mass than Original Messinger model.
(3) In three dimensional validation, there is no difference between Original Messinger model and Extended Messinger model in low inlet temperature case.
(4) In three dimensional validation, Extended Messinger model can reproduce the span direction wider icing area in the spanwise direction on the rotor fan due to the centrifugal force in high inlet temperature case.

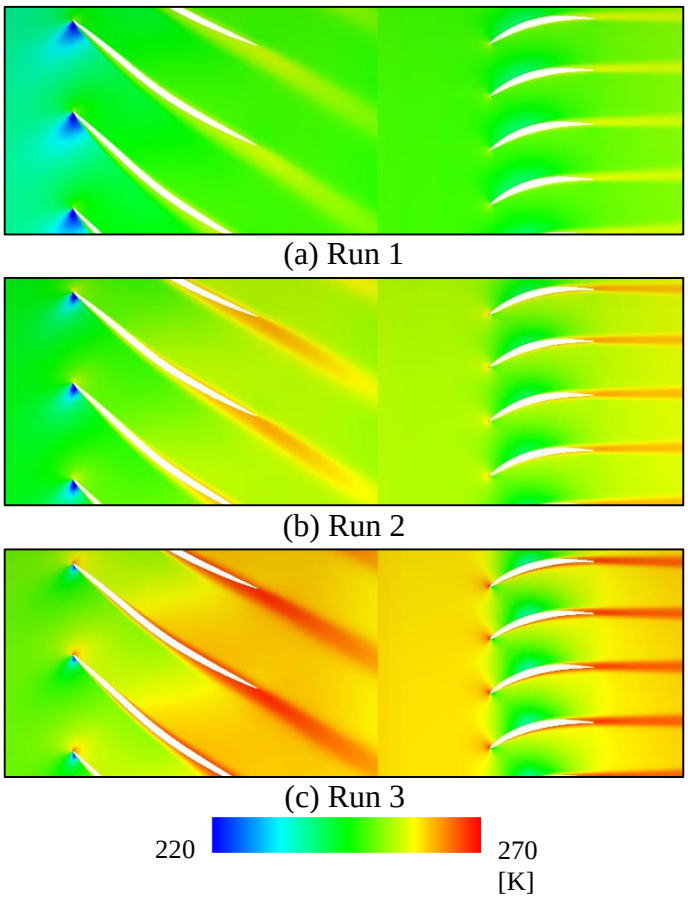

Figure 3. Static Temperature at Rotor Midspan

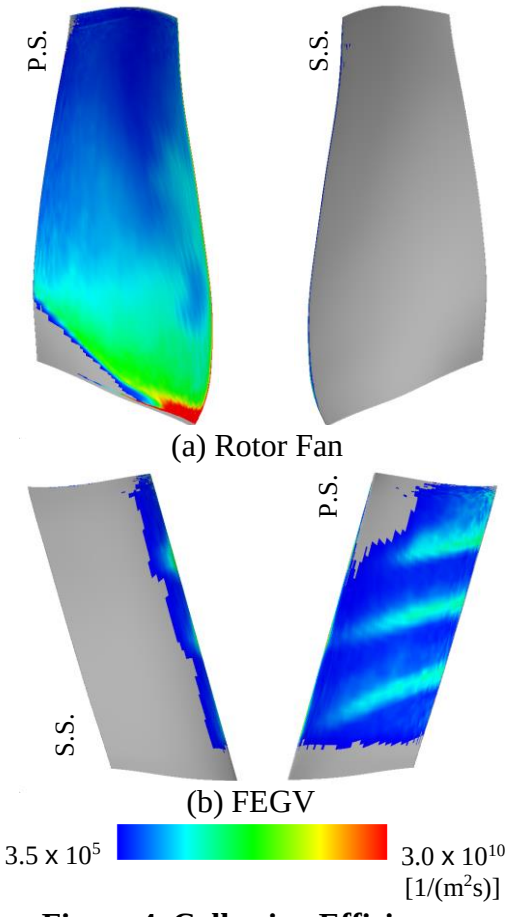

Figure 4. Collection Efficiency

(5) We recommend Extended Messinger model in simulating the icing phenomenon, because this model is superior to Original Messinger model in terms of the predictive performance of the runback mass.

References

[1] Bidwell, C. S. and Potapczuk, M. G., (1993), Users Manual for the NASA Lewice Three-Dimensional Ice Accretion Code (LEWICE3D), *NASA TM* 105974.

[2] Hedde, T. and Guffond, D., 1995, ONERA Three-Dimensional Icing Model, *Journal of AIAA*, Vol. 33, No. 6, pp. 1038–1045.

[3] Messinger, B. L., (1953), Equilibrium Temperature of an Unheated Icing Surface as a Function of Airspeed, *Jounal of the Aeronautical Sciences*, vol. 20, no.1, pp. 29-42.

[4] Kato M., Launder B. E., (1993), The modeling of turbulent flow around stationary and vibrating square cylinder, *Proceedings of 8th Symposium on Turbulent Shear Flows*, 10-4-1-10-4-6.

[5] Yee H. C., (1987), Upwind and symmetric Shock-Capturing Schemes, *NASA TM* 89464.

[6] Fujii K. and Obayashi S., (1987), Practical application of improved LU-ADI scheme for the three-dimensional Navier-Stokes computations of transonic viscous flows, *AIAA Paper*, 86-0513.

[7] Ozgen S., Canibek M., (2009), Ice accretion simulation on multi-element airfoils using extended Messinger model, *Heat and Mass Transfer*, Vol. 45, pp. 305-322.

[8] William B. Wright, P. W. Gent and Didier Gufford, (1997), DRA/NASA/ONERA Collaboration on Icing Research, *NASA CR* 202 34 9.

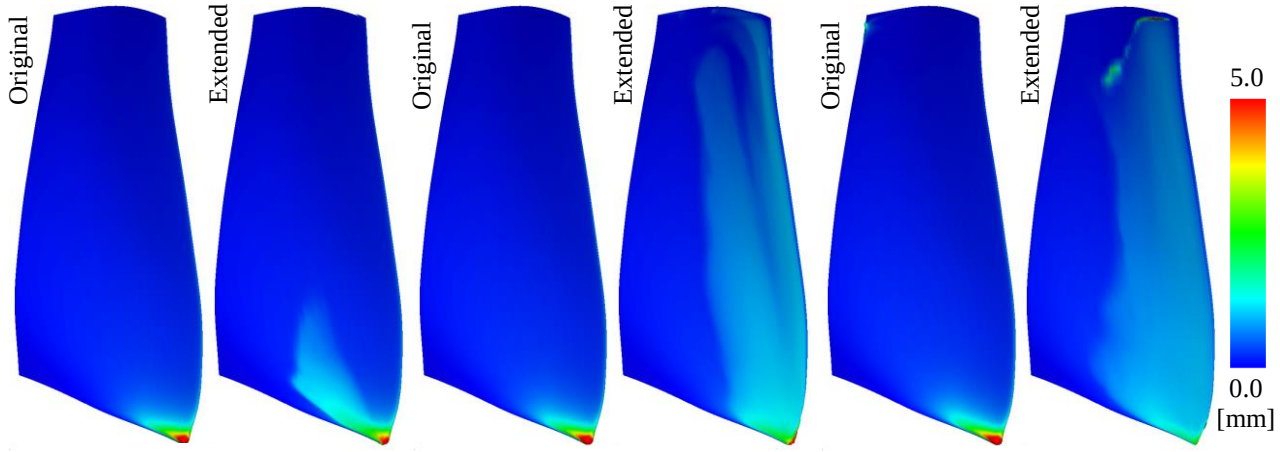

(a) Run 1 (b) Run 2 (c) Run 3

Figure 5. Ice Thickness at Suction Side of Rotor Fan

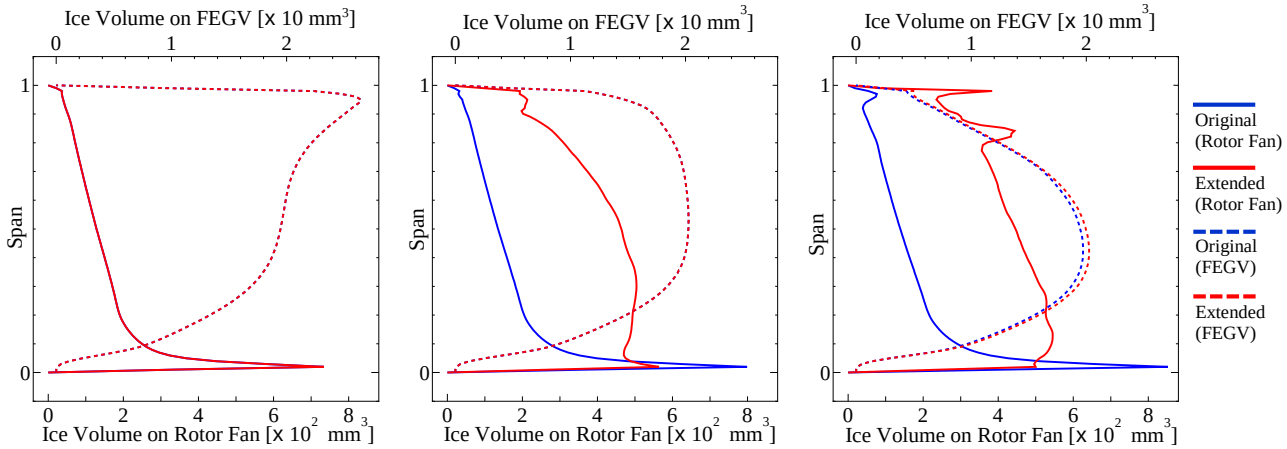

(a) Run 1 (b) Run 2 (c) Run 3

Figure 6. Ice Volume